The 6-vertex model of hydrogen-bonded crystals with bond defects



2000 J. Phys. A: Math. Gen. 33 2185

(http://iopscience.iop.org/0305-4470/33/11/302)

J. Phys. A: Math. Gen. **33** (2000) 2185–2193. Printed in the UK PII: S0305-4470(00)07335-2

# The 6-vertex model of hydrogen-bonded crystals with bond defects

N Sh Izmailian†§, Chin-Kun Hu† and F Y Wu‡

† Institute of Physics, Academia Sinica, Nankang, Taipei 11529, Taiwan
‡ Department of Physics, Northeastern University, Boston, MA 02115, USA
§ Yerevan Physics Institute, Alikhanian Br. 2, 375036 Yerevan, Armenia

Received 31 August 1999, in final form 4 January 2000

**Abstract.** It is shown that the percolation model of hydrogen-bonded crystals, which is a 6-vertex model with bond defects, is completely equivalent to an 8-vertex model in an external electric field. Using this equivalence we solve exactly a particular 6-vertex model with bond defects. The general solution for the Bethe-like lattice is also analysed.

## 1. Introduction

The 6-vertex model on a square lattice† describes hydrogen-bonded crystals in two dimensions. Historically, it was Slater [2] who first considered the evaluation of the residual entropy of ice, a hydrogen-bonded crystal, under the assumptions that (i) there is one hydrogen atom on each lattice edge, and (ii) there are always two hydrogen atoms near, and away from, each lattice site (the ice rule). Under these assumptions there are six possible hydrogen configurations at each site, and one is led to a 6-vertex model. The exact residual entropy of the 'square' ice, i.e. ice on the square lattice, was obtained by Lieb [3], which gives rise to a numerical value surprisingly close to the experimental residual entropy of real ice (in three dimensions). The 6-vertex model is therefore an accurate description of hydrogen-bonded crystals.

In real hydrogen-bonded crystals, however, bonding defects exist [4]. One way through which bond defects can occur is caused by the double-well potential seen by hydrogen atoms between two lattice sites. When two hydrogens occupy the two off-centre potential wells along a given lattice edge, assumption (i) above is broken, albeit the ice rule (ii) is still intact. This leads to the fact that one, two or zero hydrogen atoms can be present on a lattice edge. Indeed, one of the authors of this paper [5] considered this possibility in a percolation model of supercooled water. The same model was later considered by Attard and Batchelor [6] who analysed it using series analyses. More recently, Attard [7] reformulated the problem as a 14-vertex model with Bjerrum bond defects, and analysed the 14-vertex model using an independent-bond approximation. Here, using a somewhat different mapping, we establish the exact equivalence of the 6-vertex model with bond defects with an 8-vertex model in an external field. As a result, we are able to analyse the exact solution in a particular parameter subspace. We also discuss the general solution of the 6-vertex model with bond defects on the Bethe lattice.

† For a review of vertex models see [1].

0305-4470/00/112185+09$30.00  

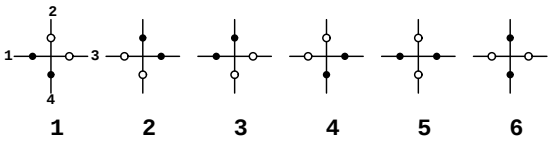


**Figure 1.** The six ice-rule configurations. Each solid circle denotes an Ising spin $\sigma = 1$ and each open circle a $\sigma = -1$.

## 2. Equivalence with an 8-vertex model

Consider a square lattice $\mathcal{L}$ of $N$ sites under periodic boundary conditions so that there are $2N$ lattice edges. The lattice is hydrogen bonded with defects such that there can be one, two or zero hydrogen atoms on each lattice edge. As the hydrogen atoms are placed off-centre on the edges, we place two Ising spins $\sigma, \sigma'$ on each lattice edge such that $\sigma = 1$ denotes that the site is occupied by a hydrogen, and $\sigma = -1$ that the site is empty. However, the ice rule dictates that the sum of the four Ising spins $\sigma_1, \sigma_2, \sigma_3, \sigma_4$ surrounding a square lattice site must vanish. Altogether there are six ice-rule configurations as shown in figure 1.

More generally, we consider the ice-rule model with weights

$$\omega_1 = \omega_2 = a \qquad \omega_3 = \omega_4 = b \qquad \omega_5 = \omega_6 = c \tag{1}$$

where $\omega_i$ is the weight of the $i$th configuration shown in figure 1. We denote the weights (1) by $\omega(\sigma_1, \sigma_2, \sigma_3, \sigma_4)$, where the subscripts are indexed as shown and $\omega_1 = \omega(1, -1, -1, 1)$, etc. The weight $\omega(\sigma_1, \sigma_2, \sigma_3, \sigma_4)$ satisfies the 'spin-reversal' symmetry

$$\omega(\sigma_1, \sigma_2, \sigma_3, \sigma_4) = \omega(-\sigma_1, -\sigma_2, -\sigma_3, -\sigma_4) \tag{2}$$

and vanishes except for the six weights given in (1). To each lattice edge containing two spins $\sigma$ and $\sigma'$, we introduce an edge factor $E(\sigma, \sigma')$ to reflect the effect of bond defects. Then, the partition function of interest is

$$Z = \sum_{\sigma=\pm 1} \prod_{\text{vertices}} \omega(\sigma_1, \sigma_2, \sigma_3, \sigma_4) \prod_{\text{edges}} E(\sigma, \sigma'). \tag{3}$$

In the 6-vertex model without bond defects we have $E(\sigma, \sigma') = (1 - \sigma\sigma')/2$, so that there is precisely one hydrogen on each lattice edge. The model considered by Attard [7] is described by

$$\begin{aligned} E(\sigma, \sigma') &= w_+ \qquad \sigma = \sigma' = 1 \\ &= w_- \qquad \sigma = \sigma' = -1 \\ &= 1 \qquad \sigma = -\sigma'. \end{aligned} \tag{4}$$

The percolation model of [5] is equivalent to a special case of (4) with $w_+ = w_- = w = \mathrm{e}^{2K}$ and

$$E(\sigma, \sigma') = \mathrm{e}^{K(\sigma\sigma'+1)} = \mathrm{e}^K (\cosh K)(1 + z\sigma\sigma') \tag{5}$$

where $z = \tanh K$. For our purposes, we shall restrict our considerations to the percolation model (5).

Attard and Batchelor [6,7] adopted an arrow representation for the hydrogen configurations which, due to the occurrence of defects, led to a 14-vertex model with Bjerrum defects. A weak-graph transformation [8] is then performed for the 14-vertex model. Here, we expand the partition function directly. Substituting (5) into (3) and expanding the second product over the edges of $\mathcal{L}$, we obtain an expansion of $2^{2N}$ terms. To each term in the expansion

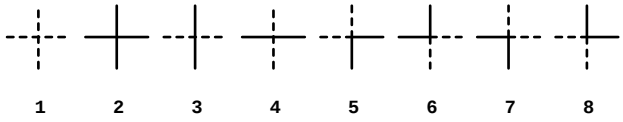


**Figure 2.** The 8-vertex model configurations.

we associate a bond graph by drawing bonds on those edges corresponding to the $z$ factors contained in the term. This leads to a 16-vertex model on $\mathcal{L}$. Besides an overall Boltzman factor $(e^K \cosh K)^{2N}$, the 16-vertex model has vertex weights

$$W = \sum_{\sigma_1\sigma_2\sigma_3\sigma_4} \left( \omega(\sigma_1, \sigma_2, \sigma_3, \sigma_4) \prod (\sqrt{z}\sigma_i) \right) \tag{6}$$

where the product is taken over those incident edges with bonds. The symmetry relation (2) now implies that $W = 0$ whenever there are an odd number of incident bonds, and the 16-vertex model becomes an 8-vertex model.

Using the bond configurations of the 8-vertex model shown in figure 2, it is straightforward to deduce, using (6), the following vertex weights:

$$\begin{aligned}
W_1 &= \sum \omega(\sigma_1, \sigma_2, \sigma_3, \sigma_4) = 2(a + b + c) \\
W_2 &= z^2 \sum \sigma_1\sigma_2\sigma_3\sigma_4\, \omega(\sigma_1, \sigma_2, \sigma_3, \sigma_4) = 2z^2(a + b + c) \\
W_3 = W_4 &= z \sum \sigma_2\sigma_4\, \omega(\sigma_1, \sigma_2, \sigma_3, \sigma_4) = 2z(-a - b + c) \\
W_5 = W_6 &= z \sum \sigma_1\sigma_2\, \omega(\sigma_1, \sigma_2, \sigma_3, \sigma_4) = 2z(-a + b - c) \\
W_7 = W_8 &= z \sum \sigma_2\sigma_3\, \omega(\sigma_1, \sigma_2, \sigma_3, \sigma_4) = 2z(a - b - c)
\end{aligned} \tag{7}$$

where $W_i$ is the vertex weight of the $i$th vertex and we have used the fact that in the non-vanishing $\omega$ we have $\sigma_1\sigma_2\sigma_3\sigma_4 = 1$. Now, in an 8-vertex model configuration, vertices 3 and 4, 5 and 6, and 7 and 8, always occur in pairs and/or in even numbers. Therefore we can conveniently replace the relevant weights by their absolute values and arrive at, after dividing all weights by a common factor $z$,

$$\begin{aligned}
W_1 &= z^{-1}(a + b + c) \\
W_2 &= z(a + b + c) \\
W_3 = W_4 &= |-a - b + c| \\
W_5 = W_6 &= |-a + b - c| \\
W_7 = W_8 &= |a - b - c|.
\end{aligned} \tag{8}$$

The vertex weights (8) describe an 8-vertex model in an external electric field $h = (\ln z)/2$ in both the vertical and horizontal directions [1].

More generally, if we allow different values of $w_+ = w_- = w_i, i = 1, 2$ in (4) and (5) for the horizontal and vertical edges respectively, and write $h = (\ln z_1)/2$ and $v = (\ln z_2)/2$, where $z_i = (w_i - 1)/(w_i + 1), i = 1, 2$, then one arrives at an 8-vertex model with weights

$$\begin{aligned}
W_1 &= e^{h+v}(a + b + c) \\
W_2 &= e^{-h-v}(a + b + c) \\
W_3 &= e^{h-v}|-a - b + c| \\
W_4 &= e^{v-h}|-a - b + c| \\
W_5 = W_6 &= |-a + b - c| \\
W_7 = W_8 &= |a - b - c|.
\end{aligned} \tag{9}$$

In ensuing discussions we shall consider the general model (9).

## 3. The free-fermion solution

The free-fermion model [9] is defined as a particular case of the 8-vertex model in which the vertex weights satisfy the relation

$$W_1W_2 + W_3W_4 = W_5W_6 + W_7W_8 \tag{10}$$

a condition equivalent to the consideration of a noninteracting many-fermion system in an $S$-matrix formulation of the 8-vertex model [10]. In the present case the free-fermion condition (10) is satisfied when either $a = 0$ or $b = 0$. Without loss of generality, we consider $a = 0$.

The closed expression for the free energy of the free-fermion model is well known [9] and after some algebraic manipulation using the results of [9], we obtain

$$-\beta f = \lim_{N\to\infty} \frac{1}{N} \ln Z = \ln(b + c) + \frac{1}{4\pi} \int_0^{2\pi} d\phi \ln(A + Q^{1/2}) \tag{11}$$

where

$$\begin{aligned} Q &= [\sinh(2v + 2h) + k^2 \sinh(2v - 2h) + 2k \cosh 2v \cos\phi]^2 + 4k^2 \sin\phi^2 \\ A &= \cosh(2v + 2h) + k^2 \cosh(2v - 2h) + 2k \sinh 2v \cos\phi \end{aligned} \tag{12}$$

with $k = |b - c|(b + c)$.

The critical condition of the free-fermion model is given by [9]

$$W_1 + W_2 + W_3 + W_4 = 2 \max\{W_1, W_2, W_3, W_4\} \tag{13}$$

where

$$\begin{aligned} W_1 &= e^{h+v}(b + c) \\ W_2 &= e^{-h-v}(b + c) \\ W_3 &= e^{h-v}|b - c| \\ W_4 &= e^{v-h}|b - c|. \end{aligned} \tag{14}$$

Thus, the $h$–$v$ plane is divided into four regions depending on which vertex 1, 2, 3 or 4 has the largest weight. Denoting the four regions by I, II, III and IV respectively, as shown in figure 3, the critical condition (13) can be rewritten as

$$\begin{aligned} \frac{b}{c} &= \frac{\tanh v + e^{2h}}{1 - e^{2h} \tanh v} && \text{region I} \\ \frac{b}{c} &= \frac{1 - e^{2h} \tanh v}{\tanh v + e^{2h}} && \text{region II} \\ \frac{b}{c} &= \frac{\tanh v - e^{2h}}{1 + e^{2h} \tanh v} && \text{region III} \\ \frac{b}{c} &= \frac{1 + e^{2h} \tanh v}{\tanh v - e^{2h}} && \text{region IV.} \end{aligned} \tag{15}$$

The critical condition (15) is plotted in figures 4(*a*)–(*d*) for four specific values of $b/c$. Generally, the free energy exhibits a logarithmic singularity at the phase boundaries with exponents $\alpha = \alpha' = 0$ [9]. When $b = c$, for which $Q$ is a complete square, however, we have

$$\begin{aligned} -\beta f &= \max\{\ln W_1, \ln W_2\} \\ &= \ln(2b) + |h + v| \end{aligned} \tag{16}$$

and the phase boundary $h + v = 0$ separates the two frozen states $W_1$ and $W_2$.

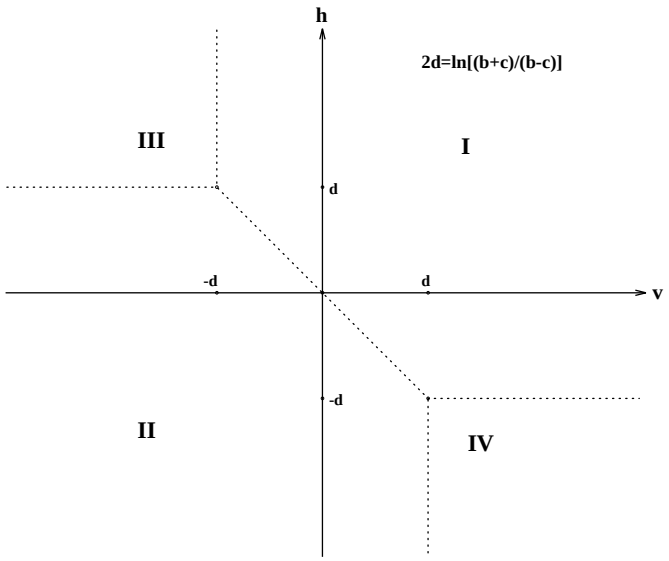


**Figure 3.** The four regions in the plane $h$–$v$ denoted by I, II, III and IV are, respectively, the regions where vertex 1, 2, 3 or 4 has lowest energy.

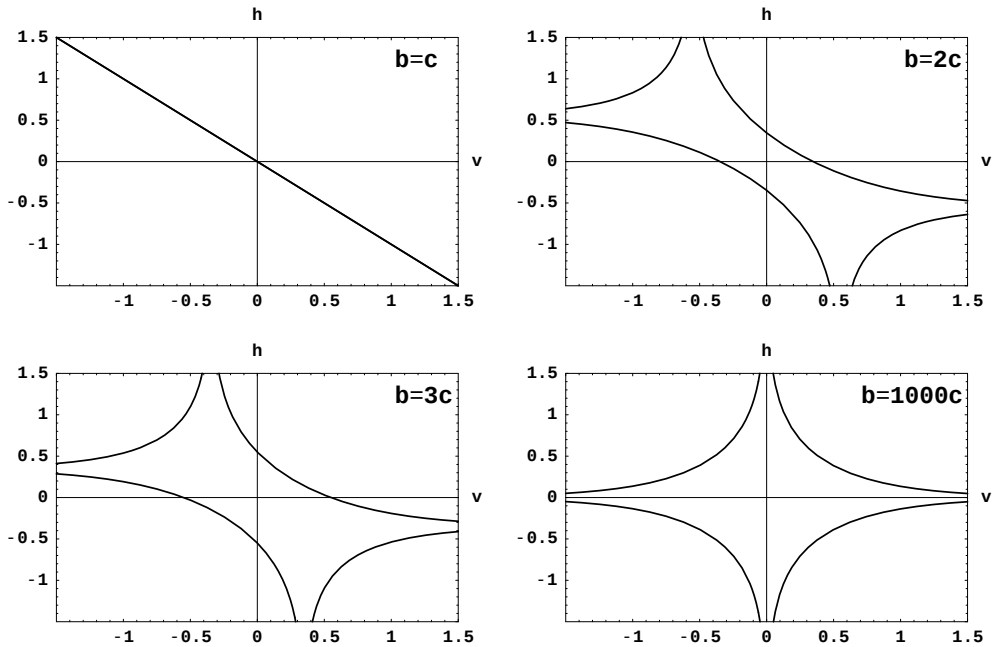


**Figure 4.** Phase boundaries of the free-fermion model.

## 4. The Bethe-like lattice

Now, we consider the 6-vertex model with bond defects on a Bethe lattice of coordination number four. As in the case of the square lattice we place two Ising spins on each lattice

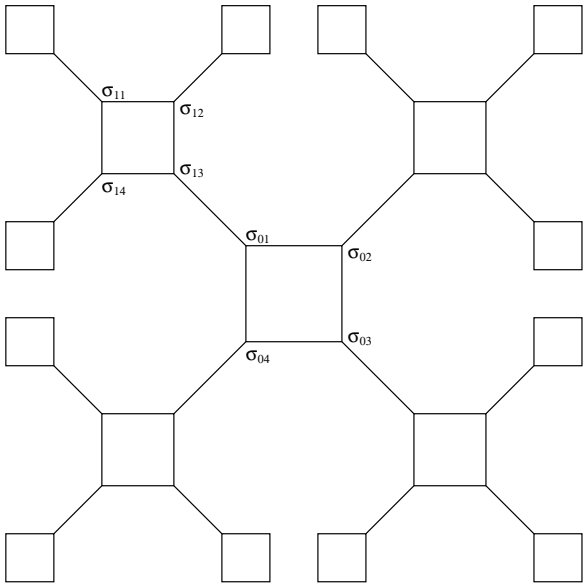


**Figure 5.** The Bethe-like lattice.

edge. Instead of dealing with the system where spins are located at the edge of the lattice we convert the Bethe lattice to a Bethe-like lattice, see figure 5, where the spins are located at the vertices, by surrounding each vertex of the Bethe lattice by a square obtained by connecting the nearest to the above-mentioned vertex spins of four edges meeting at the vertex. The study of systems in Bethe-like lattices is an alternative approach to the usual mean-field theory. The main features of the model under investigation will be obtained by studying the properties of the free energy.

The free energy in a region deep inside a Bethe-like lattice must be carefully defined. It cannot be obtained by directly evaluating the logarithm of the partition function in which the contribution from the outside of this region is not negligible, and as result the system exhibits an unusual type of phase transition without long-range order [11–13]. Recently, a method for the surface-independent free-energy calculation was presented [14, 15]. The free energy $f_{\square}$ per plaquette of our model is expressed as

$$-\beta f_{\square} = \lim_{n\to\infty} \tfrac{1}{2}(\ln Z_n - 3\ln Z_{n-1}) \tag{17}$$

where $Z_n$ and $Z_{n-1}$ are the partition functions of the 6-vertex model with bond defects on the Bethe-like lattice consisting of $n$ and $n-1$ generations, respectively.

The calculation on the Bethe-like lattice is based on a recursion method [16]. When the tree is cut at the central plaquette, it is separated into four branches, each of which contains three branches. Then the partition function of interest (3) can be written as follows:

$$Z_n = \left(\frac{w+1}{2}\right)^{N_b^{(n)}} \sum_{\{\sigma_{0i}\}} \omega(\sigma_{01},\sigma_{02},\sigma_{03},\sigma_{04}) g_n(\sigma_{01}) g_n(\sigma_{02}) g_n(\sigma_{03}) g_n(\sigma_{04}) \tag{18}$$

where $N_b^{(n)} = 2(3^n - 1)$ is the number of bonds, $n$ is the number of generations and $g_n(\sigma_{0i})$ is in fact the partition function of a branch nearest to the $0i$ site.

Each branch, in turn, can be cut along any site of the first generation, and the expressions

for $g_n(\sigma_{0i})$ can therefore be written in the form

$$g_{n+1}(\sigma_{01}) = \sum_{\{\sigma_{1i}\}} (1 + z\sigma_{01}\sigma_{13})\omega(\sigma_{11}, \sigma_{12}, \sigma_{13}, \sigma_{14}) g_n(\sigma_{11}) g_n(\sigma_{12}) g_n(\sigma_{14}). \tag{19}$$

After dividing $g_n(-)$ by $g_n(+)$, we obtain a recursion relation for $x_n = g_n(-)/g_n(+)$. Let us consider the case when a series of solutions of the recursion relation converges to a stable point at $n \to \infty$, namely,

$$\lim_{n\to\infty} x_n = x.$$

We obtain the following equation:

$$x = \frac{(1-z)x^2 + (1+z)x}{(1+z)x^2 + (1-z)x}. \tag{20}$$

All the $x_n$ are positive and therefore the stable point $x$ is also positive. We should note that the equation of state (20) has singularity at $z = -1$ (or $K = -\infty$). This case corresponds to the 6-vertex model without bond defects.

We are now in a position to compute the free energy per plaquette of our model. Using equations (17)–(20), the expression for the free-energy functional can be written as

$$\begin{aligned} -\beta f_\square = {} & \lim_{n\to\infty} \frac{1}{2}(N_b^{(n)} - 3N_b^{(n-1)}) \ln \frac{w+1}{2} \\ & + \lim_{n\to\infty} \tfrac{1}{2}[\ln \Phi(x_{(n-1)}) + \ln \Psi(x_{(n)}) - 3 \ln \Psi(x_{(n-1)})] \end{aligned} \tag{21}$$

where

$$\Psi(x) = 2(a+b+c)x^2 \qquad \text{and} \qquad \Phi(x) = (a+b+c)^4 x^4 [(1+z)x + 1 - z]^4. \tag{22}$$

It easy to see that $N_b^{(n)} - 3N_b^{(n-1)} = 4$ for all $n$. Thus the free energy per plaquette can finally be written as

$$-\beta f_\square = \ln \frac{(w+1)^2}{2}(a+b+c) + \ln \frac{(1+z)x + 1 - z}{2}. \tag{23}$$

Together with expression (20) for $x$ it gives the free energy per plaquette of the 6-vertex model with bond defects.

The equation of state (20) always has $x = 1$ as its fixed-point solution. In this case the free energy per plaquette is

$$-\beta f_\square = \ln \frac{(w+1)^2}{2}(a+b+c). \tag{24}$$

In the case of $a = b = c = 1$, we recover the result obtained by Attard and Batchelor [6] for the 6-vertex model with bond defects in the mean-field (independent-vertex) framework,

$$-\beta f_\square = \ln \tfrac{3}{2}(w+1)^2$$

which reduces to Pauling's estimate when $w = 0$ [17].

The free energy (24) for the 6-vertex model with bond defects on the Bethe-like lattice is analytical everywhere, while the vertex model on the square lattice has a very rich phase diagram, a consequence of the plethora of couplings that may be assigned to different arrow configurations and orientations. On the Bethe-like lattices orientational order is lost as there is no consistent 'up' and 'down' for a vertex. The cyclic ordering of edges round a vertex also disappears on the Bethe-like lattice. The number of couplings is thus reduced in the Bethe-like lattice with respect to the square lattice.

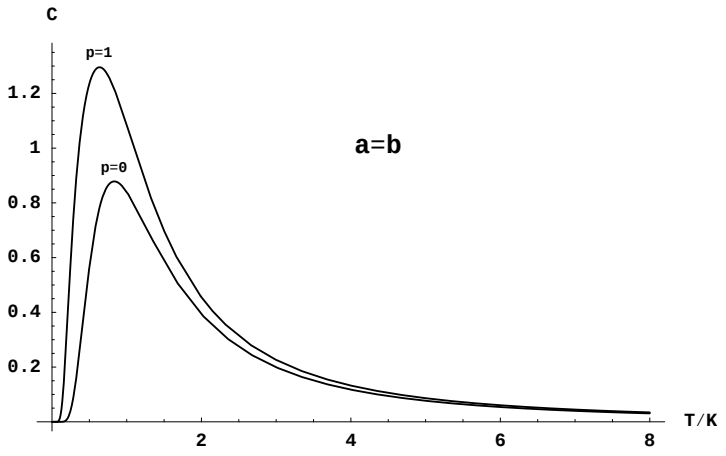


**Figure 6.** The specific heat for the Bethe-like lattice of figure 5 as function of $T/K$ for $a = b$, and for $p = (\varepsilon_a - \varepsilon_c)/K = 0, 1$.

For the specific heat, we obtain

$$C = \frac{\mathrm{d}}{\mathrm{d}T}\left[T^2\frac{\mathrm{d}}{\mathrm{d}T}(-\beta f_{\square})\right]$$
$$= \frac{2w}{(w+1)^2}(\ln w)^2 + \frac{ab(\ln a/b)^2 + ac(\ln a/c)^2 + bc(\ln b/c)^2}{(a+b+c)^2} \tag{25}$$

or, explicitly,

$$C = \frac{1}{T^2}\frac{2K^2}{(\cosh K/T)^2} + \frac{\varepsilon_{ab}^2 \mathrm{e}^{\varepsilon_{ab}/T} + \varepsilon_{ac}^2 \mathrm{e}^{\varepsilon_{ac}/T} + (\varepsilon_{ab} - \varepsilon_{ac})^2 \mathrm{e}^{(\varepsilon_{ab}+\varepsilon_{ac})/T}}{T^2(1 + \mathrm{e}^{\varepsilon_{ab}/T} + \mathrm{e}^{\varepsilon_{ac}/T})^2} \tag{26}$$

where $\varepsilon_{ab} = \varepsilon_a - \varepsilon_b$, $\varepsilon_{ac} = \varepsilon_a - \varepsilon_c$ and

$$a = \mathrm{e}^{-\varepsilon_a/T} \qquad b = \mathrm{e}^{-\varepsilon_b/T} \qquad c = \mathrm{e}^{-\varepsilon_c/T}.$$

The specific heat versus $T/K$ for $a = b$ is plotted in figure 6.

## 5. Summary and discussion

In this paper we have considered a 6-vertex model of hydrogen-bonded crystals with bond defects. We have established the exact equivalence of the 6-vertex model with bond defects with an 8-vertex model in an external electric field. Using this equivalence we exactly solve our model in the free-fermion subspace. We also obtain the exact solution of the 6-vertex model with bond defects on a Bethe-like lattice.

In [5], one of us used the percolation representation of the hydrogen-bonded model to argue that the specific heat of the system will increase as the temperature decreases from very high temperature. Figure 6 indeed shows such behaviour. However, the specific heat in figure 6 does not diverge. It is of interest to calculate the specific heat for square or diamond lattices using the Monte Carlo method. We expect to find singular specific heat behaviour in such systems.

**Acknowledgments**

This work was partly supported by the National Science Council of the Republic of China (Taiwan) under grant number NSC 89-2112-M-001-005. The work of FYW is supported in part by the National Science Foundation grant DMR-9614170. FYW thanks C K Hu for the hospitality at the Academia Sinica and T K Lee for the hospitality at the National Center for Theoretical Sciences where this work was completed.

**References**

[1] Lieb E H and Wu F Y 1972 *Phase Transitions and Critical Phenomena* vol 1, ed C Domb and M S Green (New York: Academic)
[2] Slater J C 1941 *J. Chem. Phys.* **9** 16
[3] Lieb E H 1967 *Phys. Rev. Lett.* **18** 692
[4] See for example Glasser M L 1983 *J. Stat. Phys.* **33** 753
[5] Hu C K 1983 *J. Phys. A: Math. Gen.* **16** L321
[6] Attard P and Batchelor M T 1988 *Chem. Phys. Lett.* **149** 206
[7] Attard P 1996 *Physica* A **233** 742
[8] Nagle J F 1966 *J. Math. Phys.* **7** 1484
[9] Fan C and Wu F Y 1970 *Phys. Rev.* B **2** 723
[10] Hurst C A and Green H S 1960 *J. Chem. Phys.* **33** 1059
Hurst C A 1966 *J. Math. Phys.* **7** 395
[11] Eggarter T P 1974 *Phys. Rev.* B **9** 2989
[12] Muller-Hartmann E and Zittartz J 1974 *Phys. Rev. Lett.* **33** 893
[13] Wang Y K and Wu F Y 1976 *J. Phys. A: Math. Gen.* **9** 593
[14] Gujrati P D 1995 *Phys. Rev. Lett.* **74** 809
[15] Ananikian N S, Avakian A R and Izmailian N Sh 1991 *Physica* A **172** 391
Ananikian N S, Izmailian N Sh and Oganessyan K A 1998 *Physica* A **254** 207
[16] Hu C-K and Izmailian N Sh 1998 *Phys. Rev.* E **58** 1644
Hu C-K, Izmailian N Sh and Oganesyan K B 1999 *Phys. Rev.* E **59** 6489
[17] Pauling L 1935 *J. Am. Chem. Soc.* **57** 2680